

Significance of Gravitational Nonlinearities on the Dynamics of Disk Galaxies

ALEXANDRE DEUR,¹ COREY SARGENT,² AND BALŠA TERZIĆ²

¹*Department of Physics, University of Virginia,
Charlottesville, Virginia 22901, USA*

²*Department of Physics, Old Dominion University,
Norfolk, Virginia 23529, USA*

(Received xxx; Revised yyy; Accepted zzz)

ABSTRACT

The discrepancy between the visible mass in galaxies or galaxy clusters, and that inferred from their dynamics is well known. The prevailing solution to this problem is dark matter. Here we show that a different approach, one that conforms to both the current Standard Model of Particle Physics and General Relativity, explains the recently observed tight correlation between the galactic baryonic mass and the measured accelerations in the galaxy. Using direct calculations based on General Relativity’s Lagrangian, and parameter-free galactic models, we show that the nonlinear effects of General Relativity make baryonic matter alone sufficient to explain this observation.

Keywords: general relativity – dark matter – spiral galaxies

1. INTRODUCTION

An empirical tight relation between accelerations calculated from the galactic baryonic content and the observed accelerations in galaxies has been reported by McGaugh et al. (McGaugh et al. 2016, hereafter MLS2016); larger accelerations are accounted for by the baryonic matter, i.e. there is no missing mass problem, while in lower acceleration regions, dark matter or gravitation/dynamical laws beyond Newton’s are necessary. This correlation is surprising because galactic dynamics should be dictated by the total mass (believed to be predominantly dark), but instead the baryonic mass information alone is sufficient to get the observed acceleration. A tight connection between dark and baryonic matter distributions would explain the observation, but such connection has not been expected. While the relation from MLS2016—including its small scatter—can be reproduced with dark matter models, (Ludlow et al. 2017), the consistency of the measured correlation width with the observational uncertainties suggests a dynamical origin rather than an outcome of galaxy formation, since this would add an extra component to the width.

Dynamical studies of galaxies typically use Newton’s gravity. There are however arguments that once galactic masses are considered, relativistic effects arising from large masses (rather than large velocities) may become important (Deur 2009, 2019, 2017). Their physical origin is that in General Relativity (GR), gravity fields self-interact. In this article, we explore whether these effects can explain the relation in MLS2016 without requiring dark matter or modifying gravitation as we currently know it.

The article is organized as follows. We first outline the self-interaction effects in GR. Then we discuss in Section 3 the empirical tight dependence of observed acceleration on baryonic mass in disk (i.e. lenticular and spiral) galaxies. In Section 4, we use GR’s equations to compute the correlation. These CPU-intensive calculations allow us to study only a few galaxies, modeled as bulge-less disks. To cover the full range of disk galaxy morphologies, including those with significant bulge, we develop in Section 5 two dynamical models of disk galaxies in different but complementary ways: uniform sampling (Section 5.1) and random sampling (Section 5.2) of the galactic parameter space. In Section 6 we show the results from these models, and compare them to observations. Finally, in Section 7, we summarize our findings and their importance.

2. SELF-INTERACTION EFFECTS IN GENERAL RELATIVITY

Field self-interaction makes GR non-linear. The phenomenon is neglected when Newton’s law of gravity is used, as typically done in dynamical studies of galaxies or galaxy clusters. However, such a phenomenon becomes significant once the masses involved are large enough. Furthermore, it is not suppressed by low velocity—unlike some of the more familiar relativistic effects—as revealed by e. g. the inspection of the post-Newtonian equations (Einstein et al. 1938). In fact, the same phenomenon exists for the strong nuclear interaction and is especially prominent for slow-moving quark systems (heavy hadrons), in which case it produces the well-known quark confining linear potential.

The connection between self-interaction and non-linearities is seen e.g. by using the polynomial form of the Einstein-Hilbert field Lagrangian (see e.g. Salam 1974; Zee 2013)

$$\mathcal{L} = \frac{\sqrt{\det(g_{\mu\nu})} g_{\mu\nu} R^{\mu\nu}}{16\pi G} = \sum_{n=0}^{\infty} (16\pi GM)^{n/2} [\varphi^n \partial\varphi\partial\varphi] \quad (1)$$

where $g_{\mu\nu}$ is the metric, $R_{\mu\nu}$ the Ricci tensor, M the system mass and G is the gravitational constant. In the natural units ($\hbar = c = 1$) used throughout this article, $[G] = \text{energy}^{-2}$. The polynomial is obtained by expanding $g_{\mu\nu}$ around a constant metric $\eta_{\mu\nu}$ of choice, with $\varphi_{\mu\nu} \equiv g_{\mu\nu} - \eta_{\mu\nu}$ the gravitational field. The brackets are shorthands for sums over Lorentz-invariant terms (Deur 2017). Field self-interaction originates from the $n > 0$ terms in Eq. (1), distinguishing GR from Newton’s theory, for which the Lagrangian is given by the $n = 0$ term. One consequence of the $n > 0$ terms is that they effectively increase gravity’s strength. It is thus reasonable to investigate whether they may help to solve the missing mass problem. In fact, it was shown that they allow us to quantitatively reproduce the rotation curves of galaxies and the dynamics of clusters without need for dark matter, also providing a natural explanation for the flatness of the rotation curves (Deur 2009).

The phenomenon underlying these studies is ubiquitous in Quantum Chromodynamics (QCD, the gauge theory of the strong interaction). The GR and QCD Lagrangians are similar and both contain field self-interaction terms. In QCD, their effect is well-known as they are magnified by the large QCD coupling, typically $\alpha_s \approx 0.1$ at the transition between perturbative and strong regimes (Deur et al. 2016). In GR, self-interaction becomes important for non-negligible values of the coupling $\sqrt{GM/L}$ (L is the system’s characteristic scale, used here to form the dimensionless coupling needed to heuristically assess self-interaction’s importance), typically for $\sqrt{GM/L} \gtrsim 10^{-3}$ (Deur 2017). In QCD, a critical effect of self-interaction is a stronger binding of quarks, resulting in their confinement. In GR, self-interaction likewise increases gravity’s strength, which can explain the missing mass problem (Deur 2009).

One may question the relevance of field self-interaction at large galactic radii r , where on the one hand the matter density is small, so field self-interaction is negligible, and where the matter density is small, so field self-interaction is negligible, but where the missing mass problem grows worst. However, once the gravity field lines are distorted at small r due to large matter density there, they evidently remain so even if the matter density becomes negligible (no more field self-interaction, i.e. no further distortion of the field lines), preserving a form of potential different to that of Newton. Thus, even if the gravity field becomes weak, the deviation from Newton’s gravity remains¹.

A key feature for this article is the suppression of self-interaction effects in isotropic and homogeneous systems (Deur 2009):

- In a two-point system, large $\sqrt{GM/L}$ or α_s values lead to a constant force between the two points (and a vanishing force elsewhere), i.e. the string-like flux-tube, well-known in QCD.
- For a homogeneous disk, because of the symmetry, the flux collapses only outside the disk plane. The resulting force between the disk center and a point in the disk at distance r decreases as $1/r$.
- For a homogeneous sphere, the force recovers its usual $1/r^2$ behavior since the flux has no particular direction or plane of collapse.

This symmetry dependence has led to the discovery of a correlation between the missing mass of elliptical galaxies and their ellipticity (Deur 2014). This also illustrates the point of the previous paragraph: even if the matter density in the disk decreases quickly with r , the missing mass problem—which in our approach comes from the difference between the GR and Newtonian treatments—grows worst since the difference between the $1/r$ GR force in the 2D disk and the $1/r^2$ Newtonian force grows with r . This offers a simple explanation for the relation reported in MLS2016:

¹ An analogous phenomenon exists for QCD: the parton distribution functions (PDFs) that characterize the structure of the proton are non-perturbative objects even if they are defined and measured in the limit of the asymptotic freedom of quarks where α_s tends to zero. Thus, PDFs are entirely determined by the self-interaction/non-linearities of QCD, although those are negligible at the large energy-momentum scale where PDFs are relevant.

although densities, and thus accelerations, are largest at small r , the $1/r - 1/r^2$ difference between the GR and Newtonian treatments remains moderate. However, it becomes important at large r although accelerations are small. Furthermore, at small r , the $1/r^2$ force is restored for GR due to finite disk thickness h_z , since isotropy is restored for $r \lesssim h_z$. Moreover, since disk galaxies often contain a central high-density bulge that is usually nearly spherical (Méndez-Abreu et al. 2008), self-interaction effects are suppressed there by the near-spherical symmetry, and the departure from the $1/r^2$ behavior occurs after the bulge-disk transition.

3. BARYONIC MASS—ACCELERATION DEPENDENCE

The correlation between the radial acceleration traced by rotation curves (g_{obs}) and that predicted by the known distribution of baryons (g_{bar}) reported in MLS2016 was established after analyzing 2693 points in 153 disk galaxies with varying morphologies, masses, sizes, and gas fractions. The MLS2016 authors found a good functional form fitting the correlation:

$$g_{\text{obs}} = \frac{g_{\text{bar}}}{1 - e^{-\sqrt{g_{\text{bar}}/g_{\dagger}}}}, \quad (2)$$

where g_{\dagger} is an acceleration scale, the only free parameter of the fit. In the remainder of the article, we show that the observed correlation may entirely be due to the nonlinear GR effects which are neglected in the traditional Newtonian analysis. In the next section, we use the results of direct GR calculations of rotation curves of actual galaxies modeled as bulge-less disks (Deur 2009). We show that when the galactic bulge of the actual galaxy is negligible, the calculation yields a relation that agrees with the empirical correlation from MLS2016. In the two subsequent sections, we develop models to include the effect of bulges and to account for the variation of morphology of disk galaxies.

4. DIRECT CALCULATIONS

The rotation curves of several disk galaxies were computed in (Deur 2009) based on Eq. (1) and using numerical lattice calculations in the static limit (Deur 2017). These calculations neglect the galactic bulge and approximate a spiral galaxy with a disk featuring an exponentially-falling density profile. They were carried out for nearly bulge-less Hubble types 5 and 6 galaxies (NGC 2403, 3198 and 6503), and for Hubble types 3 and 4 galaxies (NGC 2841, 2903 and 7331), which have moderate bulges. Using these results, we can compute the total acceleration g_{SI} stemming from baryonic matter and including GR's field self-interaction—analogue of g_{obs} from MLS2016. Plotting it versus the Newtonian acceleration g_{N} obtained from the same distribution of baryonic matter, but ignoring GR's self-interaction—analogue of g_{bar} from MLS2016—one obtains the results shown in the top panel of Fig. 1. The curves for types 5 and 6 galaxies agree well with the observed correlation, thereby providing an explanation for it in bulge-less galaxies. However, the curves for types 3 and 4 galaxies, while qualitatively following the correlation, overestimate g_{SI} and lie on the edge of the observed distribution. That the empirical correlation is reproduced only for bulge-less galaxies supports that 1) the correlation from MLS2016 is explainable by GR's self-interaction without requiring dark matter or modification of the known laws of Nature, and 2) at large acceleration, i.e. typically for small galactic radii, the bulge reduces the value of g_{SI} since self-interaction effects cancel for isotropically distributed matter.

Although based directly on the GR's Lagrangian, the lattice approach is limited since it is computationally costly—restricting the study to a few galaxies—and it applies only to simple geometry—limiting the studied galaxies to late Hubble types. To study the correlation from MLS2016 over the wide range of disk galaxy morphologies, we developed two models based on: 1) the $1/r$ gravitational force resulting from solving Eq. (1) for a disk of axisymmetrically distributed matter; and 2) the expectation that GR field self-interaction effects cancel for spherically symmetric distributions, such as that of a bulge, restoring the familiar $1/r^2$ force.

5. DYNAMICAL MODELS

To circumvent the limitations of the direct lattice calculation, we constructed two elementary models for disk galaxies. They both compute the acceleration including GR's self-interaction, g_{SI} , and the Newtonian acceleration due to the baryonic matter, g_{N} . Both g_{SI} and g_{N} are computed at a set of radii r , from the galactic center to its outermost parts. This is carried out for galaxies with parameters sampling the observed correlations reported in literature.

The modeled galaxies have two components: a spheroidal bulge and a larger disk. Both contain only baryonic matter following the light distribution, i.e. there is no dark matter and gas is either neglected or follow the stellar distribution.

The bulge is modeled with the projected surface brightness Sérsic profile (Sérsic 1963) used in (Méndez-Abreu et al. 2008): $I_b(R) = I_e 10^{-b_n[(R/R_e)^{1/n} - 1]}$, where R is the projected radius, I_e is the surface brightness at the half-light radius

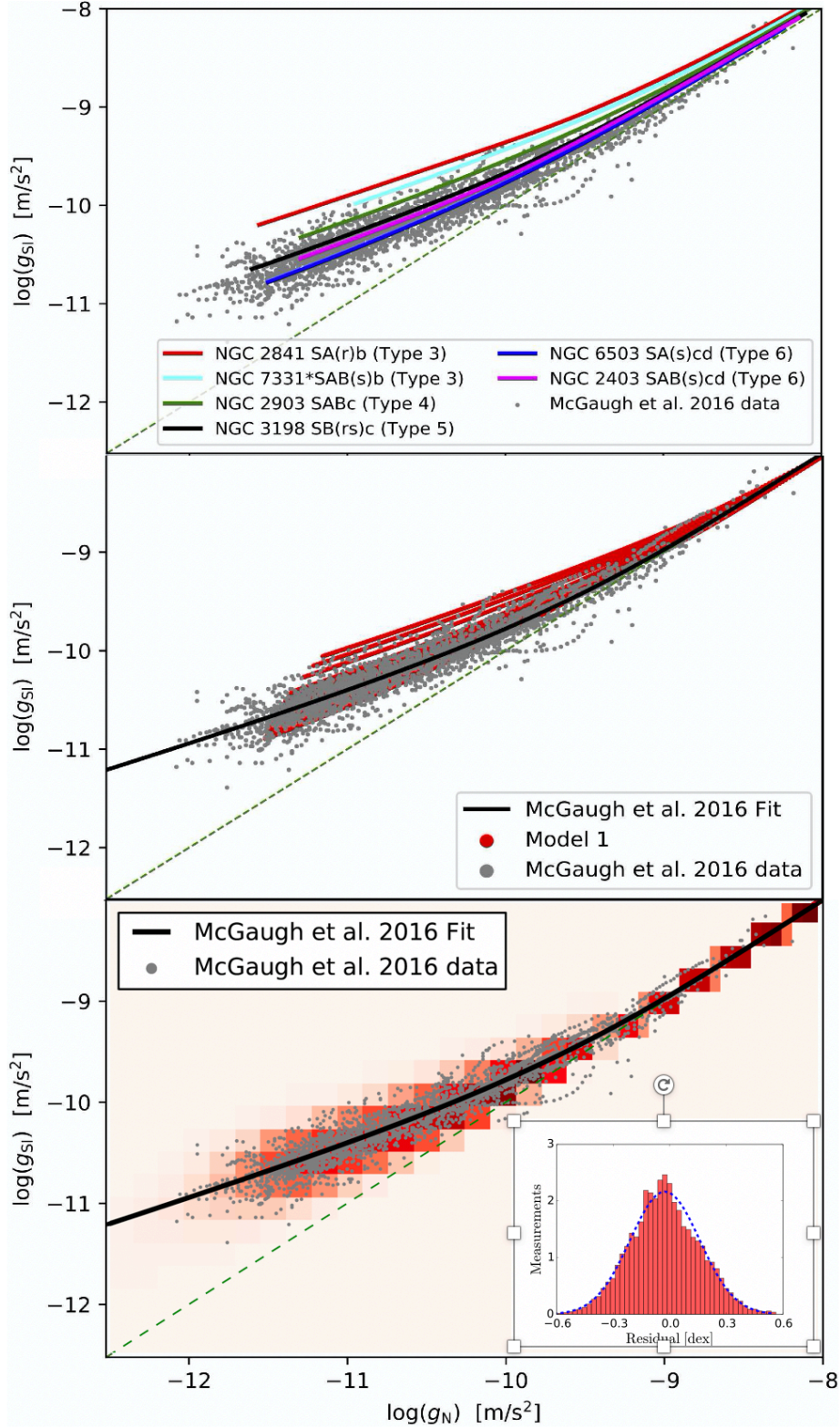


Figure 1. Correlation between the acceleration accounting for GR’s self-interaction, g_{SI} , and the acceleration computed with Newtonian gravity, g_N , plotted along with the correlation observed in MLS2016 (grey circles). Top: Lagrangian-based calculations for various Hubble type galaxies. The galaxies are approximated as pure (bulge-less) disks. The calculations agree well with observation when this approximation is justified (types 5 and 6 galaxies) but depart gradually from observation as the bulge becomes more important. Middle: Model 1 with uniform sampling of the galactic parameter phase space. Bottom: Model 2 with galactic parameter phase space sampled following observed distributions (1146 galaxies, sampled at 100 radial values are shown). The density of the data points obtained with Model 2 is encoded by the color scale. The dashed line indicates $g_{SI} = g_N$. Embedded in the bottom panel is the residual distribution between the result of Model 2 and the best fit to the observational data (black line).

R_e , n is the Sérsic parameter and $b_n \approx 0.868n - 0.142$ (Caon et al. 1993). The internal mass density $\rho_b(r)$, where r is the deprojected radius, is computed from the surface brightness by numerically solving the Abel integral. Since GR's self-interaction effects cancel for isotropic homogeneous distributions, the potential in the bulge has the usual Newtonian form, $\Phi_b(r) = GM_b^{\text{enc}}(r)/r$, where $M_b^{\text{enc}}(r)$ is the bulge mass enclosed within a sphere of radius r .

The disk is modeled with the usual surface brightness radial profile $I_d(R) = I_0 e^{-R/h}$, where I_0 is the central surface brightness, h is the disk scale length, and possible effects from the disk thickness are neglected. Again, the corresponding mass density $\rho_d(r)$ is computed from the Abel integral. Self-interaction in a homogeneous disk leads to a potential $\Phi_d(r) = G'M_d^{\text{enc}}(r) \ln(r)$, with $M_d^{\text{enc}}(r)$ the disk mass enclosed within a radius r , and G' the effective coupling of gravity in two dimensions, which depends on the physical characteristics of the disk (Deur 2017); see detailed discussion in the appendix.

The parameters characterizing a galaxy—the bulge and disk masses, M_b , M_d (from which $\rho_{b,0}$ and $\rho_{d,0}$ are obtained, respectively), R_e , n and h —span their observed ranges for S0 to Sd galaxies (Méndez-Abreu et al. 2008; Graham & Worley 2008; Sofue 2015). There are known relations between these parameters (Méndez-Abreu et al. 2008; Sofue 2015):

$$\log(R_e) = 0.91(7) \log(h) - 0.40(3), \quad (3)$$

$$\log(n) = 0.18(5)R_e + 0.38(2), \quad (4)$$

$$\log(M_d) = 0.58(32) \log(M_b) + 0.002(79). \quad (5)$$

We use values of R_e and M_b from the ranges of observed values to obtain the remaining galactic parameters— h , n , M_d —through Eqs. (3)-(5). Thus, there are no adjustable parameters in our models.

We stress that the accuracy of the empirical relations Eqs. (3)-(5) is not critical to this work, their purpose being only to provide reasonable values of the galactic parameter space we select. While the simplicity of our models would make it of limited interest for investigating the intricate peculiarities of galaxies, such simplicity is beneficial for the present study: no numerous parameters nor phenomena (e.g. baryonic feedback) are needed for adjustment to reproduce the correlation from MLS2016. That the correlation emerges directly from basic models underlines the fundamental nature of the correlation.

The two dynamical models introduced in the remainder of this section share the above description. From here, they differ in two aspects. The first is in how the observed correlations in Eqs. (3)-(5) are implemented: Model 1 enforces the correlations strictly, while Model 2 allows for the parameter space to be randomly sampled. The second difference is in representing the transition between the bulge-dominated regime near the center and disk-dominated regime.

5.1. Model 1: Uniform Sampling of the Galactic Parameter Space

This model generates a galaxy set representative of disk galaxy morphologies by uniformly sampling the values of the galactic parameters discussed in the previous Section. The model strictly enforces Eqs. (3)-(5). This offers the advantage of simplicity, e.g. clarity, speed and robustness. Actual correlations, however, vary in their strengths. Hence, strictly implementing a correlation between parameters a and b , and another between a and c , would result in parameters b and c being also correlated, while if the actual correlations between a and b , and a and c are both weak, then b and c may not be correlated. For example, propagating correlations among different galactic parameters yields an inadequate relation between M_b and M_d : $M_d \propto M_b^{-\alpha \pm \Delta}$, with $\Delta \gg \alpha = 31$. To circumvent this problem, we use $h \propto R_e^{1.0}$, $M_b \propto R_e^{0.1}$, $n \propto R_e^{0.1}$ and $M_d \propto h^{1.0}$, in rough agreement with the correlations from Refs. (Méndez-Abreu et al. 2008; Khosroshahi et al. 2000).

The correlations are applied strictly, i.e. without accounting for the scatter seen in actual data, since systematically spanning the observed typical ranges for the parameters contributes to the width of the correlation reported in MLS2016, and accounting for such scatter would partly double-count, and thus overestimate, the width.

Inside the spherical bulge-dominated region ($r < r_t$; denoted by subscript $r < r_t$), the self-interaction cancels, and the GR and Newtonian accelerations are the same:

$$g_{\text{sl}, r < r_t}(r) = g_{\text{N}, r < r_t}(r) = \frac{G}{r^2} (M_b^{\text{enc}}(r) + M_d^{\text{enc}}(r)), \quad (6)$$

where

$$M_b^{\text{enc}}(r) = 4\pi \int_0^r \tilde{r}^2 \rho_b(\tilde{r}) d\tilde{r}, \quad (7)$$

$$M_d^{\text{enc}}(r) = 2\pi \int_0^r \tilde{r} \rho_d(\tilde{r}) d\tilde{r}. \quad (8)$$

In the disk-dominated region ($r > r_t$; denoted by subscript $r > r_t$), numerical lattice calculations indicate that self-interaction leads to a collapse in the gravitational field lines (Deur 2009, 2017). The bulge density there is less significant than that of the disk, but is still present. The total acceleration is:

$$g_{\text{sl}, r > r_t}(r) = \frac{G}{r^2} M_b^{\text{enc}}(r) + \frac{G'}{r} M_d^{\text{enc}}(r). \quad (9)$$

The Newtonian acceleration $g_{\text{N}, r > r_t}$ in this region retains the form given in Eq. (6).

G' is determined by requiring the accelerations to match at r_t : $g_{\text{sl}, r < r_t}(r_t) = g_{\text{sl}, r > r_t}(r_t)$. Thus, $G' = G/r_t$, by construction. The justification for this choice of G' is explained in detail in the appendix.

The accelerations in the bulge and disk regions are smoothly connected using a Fermi-Dirac function centered at $r_t = 2R_e$ and of width $r_t/2$: $D(r) = 1/(1 + e^{2(r-r_t)/r_t})$. Therefore, the acceleration with self-interaction is:

$$g_{\text{sl}}(r) = D(r)g_{\text{sl}, r < r_t}(r) + (1 - D(r))g_{\text{sl}, r > r_t}(r), \quad (10)$$

while the Newtonian acceleration is:

$$g_{\text{N}}(r) = \frac{G}{r^2} (M_b^{\text{enc}}(r) + M_d^{\text{enc}}(r)). \quad (11)$$

The choice of width value for $D(r)$ influences little the result: abruptly transitioning between bulge and disk, i.e. using a step-function rather than $D(r)$, yields quantitatively similar results. The small dependence on the functional form for the transition is also supported by the agreement between Models 1 and 2 which use different methods for the transition, as we discuss next.

5.2. Model 2: Random Sampling of the Galactic Parameter Space

For Model 2, we randomly generate the galaxy parameters with gaussian distributions centered at the observed parameter values, and of widths determined by the observed distributions. In order to sample a realistic galaxy parameter space, we apply two types of cuts on the generated galaxy parameters. The first type of cut ensures that the randomly sampled galaxy parameters simultaneously satisfy Eqs. (3)-(5). A candidate galaxy is generated by first randomly sampling a distribution of R_e , and then using it to randomly sample the observed correlations in Eqs. (3)-(4) to obtain h and n . These are then combined with Eq. (5) to find $\rho_{b,0}$ and $\rho_{d,0}$, thereby completing the parameter set for a single candidate galaxy. This particular candidate galaxy then passes the first cut if its parameters satisfy all of the correlations to within one standard deviation. Galaxies which pass this first cut are shown as orange and red circles in Fig. 2. The second type of cut is outlined below.

The transition between the bulge- and the disk-dominated regions are implemented with a step-function $H(x) = 1$ for $x < 0$, and 0 otherwise, such that at r_t , the acceleration is kept continuous by the proper choice of G' . The transition radius r_t is defined as the radial location at which the acceleration due to the disk alone is equal to that due to the bulge alone:

$$G \frac{M_b^{\text{enc}}(r_t)}{r_t^2} = G' \frac{M_d^{\text{enc}}(r_t)}{r_t}, \quad (12)$$

with $G' = G/r_t$ (see appendix). This choice of G' simplifies the condition for the transition r_t to

$$M_b^{\text{enc}}(r_t) = M_d^{\text{enc}}(r_t). \quad (13)$$

Some bulge-dominated galaxies will not have such a transition within $r = 100$ kpc, and are removed from the sample. This is the second type of cut applied on the parameter space. Galaxies that pass both the first and the second types of cuts are shown as red circles in Fig. 2. Essentially, orange circles denote galaxies that are largely bulge-dominated and thus cannot qualify as disk galaxies. The red circles are for galaxies with small to moderate bulge that qualify as disk galaxies.

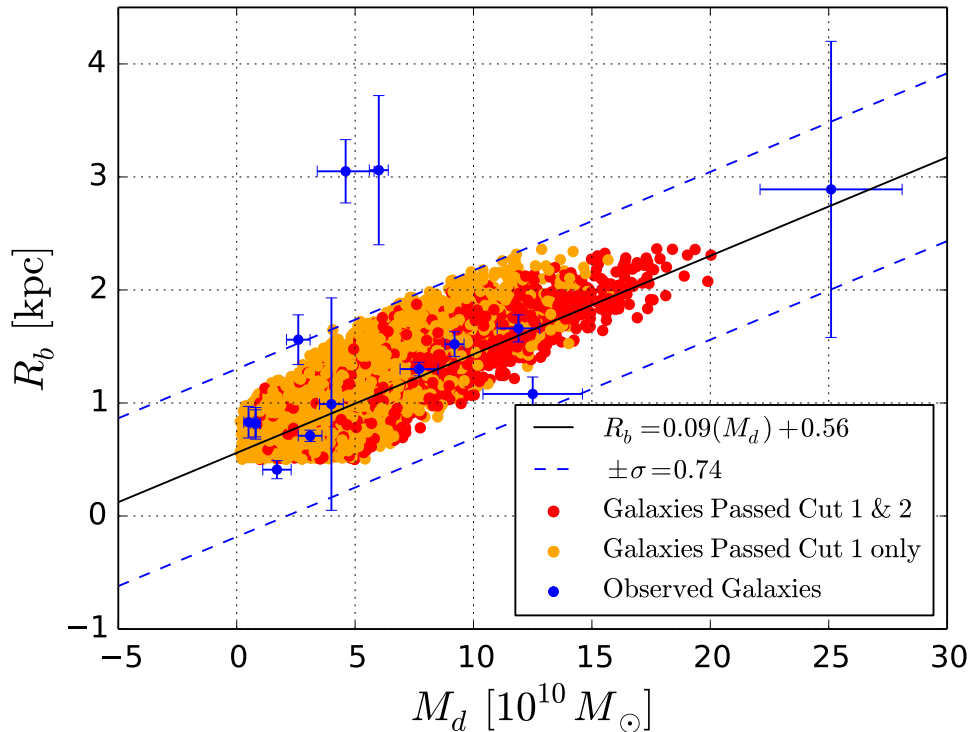


Figure 2. R_b vs. M_d . Observed values are shown as blue diamonds (Sofue 2015). The best χ^2 fit to the observed data is denoted with a solid line, and one dex in dashed lines. Orange circles denote generated galaxies which passed the first type of cut only, and red circles galaxies which passed both types of cuts. The galaxies signaled by the red circles are disk galaxies, while those corresponding to the orange circles are too bulge-dominated to qualify as such.

Models 1 and 2 use different methods for the bulge-disk transition. The agreement between the two models suggests that they are indifferent to a particular method. The acceleration including self-interaction is

$$g_{\text{sl}}(r) = H(r - r_t)g_{\text{sl},r < r_t}(r) + (1 - H(r - r_t))g_{\text{sl},r > r_t}(r), \quad (14)$$

where $g_{\text{sl},r < r_t}(r)$ and $g_{\text{sl},r > r_t}(r)$ are given in Eqs. (6)-(9) and $g_{\text{N}}(r)$ in Eq. (11).

In Model 2, we also modeled the effect of the bulge being spheroidal rather than spherical by introducing a polar dependence: $\rho_b(r, \phi) = \rho_b(r)(1 - \epsilon \cos^2 \phi)$, with $\rho_b(r)$ the spherical bulge density used in Models 1 and 2. This refinement did not noticeably change the results, thereby further proving their robustness.

6. RESULTS

Direct lattice calculation and the two dynamical models allow us to compute the accelerations for a set of galaxies whose parameters follow the typical observed ranges for disk galaxies. The acceleration including non-linear self-interaction (g_{sl}) is plotted in Fig. 1 versus the acceleration computed with the same baryonic mass distribution but assuming Newtonian gravity (g_{N}). This is compared to the observed correlation between g_{obs} and g_{bar} reported in MLS2016. The top panel shows the results for the direct calculation, the middle panel the results for Model 1, and bottom panel for Model 2. Since Model 2 samples the full parameter space selected by the cuts, but with statistical weights favoring the more probable parameter space loci, the results must be plotted as data point densities. In Fig. 1 bottom panel, the higher densities are indicated by the darker colors. Our computed correlations agree well with the empirical observation, without invoking dark matter or new laws of gravity/dynamics. The residual distribution between the result of Model 2 and the best fit to the observational data, given by Eq. (2), is shown in the embedded figure in the bottom panel of Fig. 1. (Since Model 1 samples the galactic phase space uniformly rather than using normal distributions, a residual would have little meaning.)

7. DISCUSSION AND CONCLUSION

Our findings support the possibility that GR's self-interaction effects increase the gravitational force in large, non-isotropic mass distributions. When applied to disk galaxies, the increased force on the observed matter transposes to the missing mass needed in the traditional Newtonian analyses. We have thus proposed a plausible explanation for the correlation between the luminous mass in galaxies and their observed gravitational acceleration shown in MLS2016. That this correlation is encapsulated in our basic, parameter-free, models indicates its fundamental origin.

The explanation proposed here is natural in the sense that it is a consequence of the fundamental equations of GR and of the characteristic magnitudes of the galactic gravitational fields, and in the sense that no fine tuning is necessary. This contrasts with the dark matter approach that necessitates both yet unknown particles and a fine tuning in galaxy evolution and baryon-dark matter feedbacks (see e.g. Ludlow et al. 2017). We used several approaches that are quite different, thus leading to a robust conclusion.

The work presented here adds to a set of studies that provide straightforward and natural explanations for the dynamical observations suggestive of dark matter and dark energy, but without requiring them nor modifying the known laws of Nature. This includes flat rotation curves of galaxies (Deur 2009), the Bullet cluster (Clowe et al. 2006; Deur 2009), galaxy cluster dynamics (Deur 2009), and the evolution of the universe (Deur 2019). The Tully-Fisher relation (Tully & Fisher 1977) also finds an immediate explanation (Deur 2009). There are compelling parallels between those observations and QCD phenomenology, e.g. the equivalence between galaxies' Tully-Fisher relation, and hadrons' Regge trajectories (Deur 2009, 2017), plausibly due to the similarity between GR's and QCD's underlying fundamental equations. The fact that these phenomena are well-known for other areas of Nature that possess a similar basic formalism; the current absence of natural and compelling theory for the origin of dark matter (supersymmetry being now essentially ruled out); and the yet unsuccessful direct detection of a dark matter candidate or its production in accelerators despite coverage of the phase-space expected for its characteristics; all support the approach we present here as a credible solution to the missing mass problem.

ACKNOWLEDGEMENTS

We are grateful to S. McGaugh for kindly sharing the raw data from his publication. This work is done in part with the support of the U. S. National Science Foundation award No. 1535641 and No. 1847771.

APPENDIX: NON-UNIVERSALITY OF G' AND ITS VALUE FOR INFINITELY THIN DISKS

The expression of the gravitational force confined in 2D is $G'Mm/r$. Therefore, one would naturally expect G' to be universal, like G in the 3D case. Furthermore, in the analogous QCD case, the effective coupling σ (the analog of G'), known as the QCD string tension, is indeed universal with a value of 0.18 GeV^2 (Deur et al. 2016). However, G' is not universal, but depends on the geometry of the galaxy, its mass, and its density distribution.

To understand why, it is convenient to visualize a force as a field flux through an elementary surface. The force coupling constant controls the overall density of the field lines for a unit of charge or mass. Its value does not change the r -dependence of the force². Likewise, G' determines the overall density of field lines passing through an elementary segment. This density depends on how early the transition from 3D to 2D occurs, as sketched in Fig. 3, where, for clarity, we have drawn only the field lines emerging from the center of the galaxy, its densest locus. The transition occurs early for large disk densities, or can be delayed by the presence of a spherically symmetric bulge. Therefore, G' depends on both the morphology and mass distribution of the galaxy components. In the case of an early transition (red lines in Fig. 3), the field lines are denser and G' is large. For a later transition (blue lines), the field lines are sparser and G' is smaller. Thus, G' is not universal and approximately obeys $G' = G/r_t$.

In the QCD case, σ is universal because there is no geometrical or color charge variation: for the heavy meson case to which σ applies, two static pointlike sources of unit color charge are invariably considered, with the flavors of the sources and their type of color having no influence on the force. Therefore the same distortion of field lines occurs, regardless of the type of meson considered, and σ is universal.

One may also ask what is the value of G' for a pure (bulge-less) disk, since there is no bulge-to-disk transition. Inside the disk, the mass distribution is approximately isotropic so the scale height h_z of the disk sets a first limit for the scale: one expects $r_t \propto h_z$. However, considering an infinitely thin disk reveals that a transition scale r_t emerges

² This is true only in the classical case. Running couplings in quantum field theory do affect the r -dependence because short distance quantum effects are folded into the definition of the coupling (Deur et al. 2016). This definition of the coupling at quantum scale is conventional and, in any case, irrelevant here.

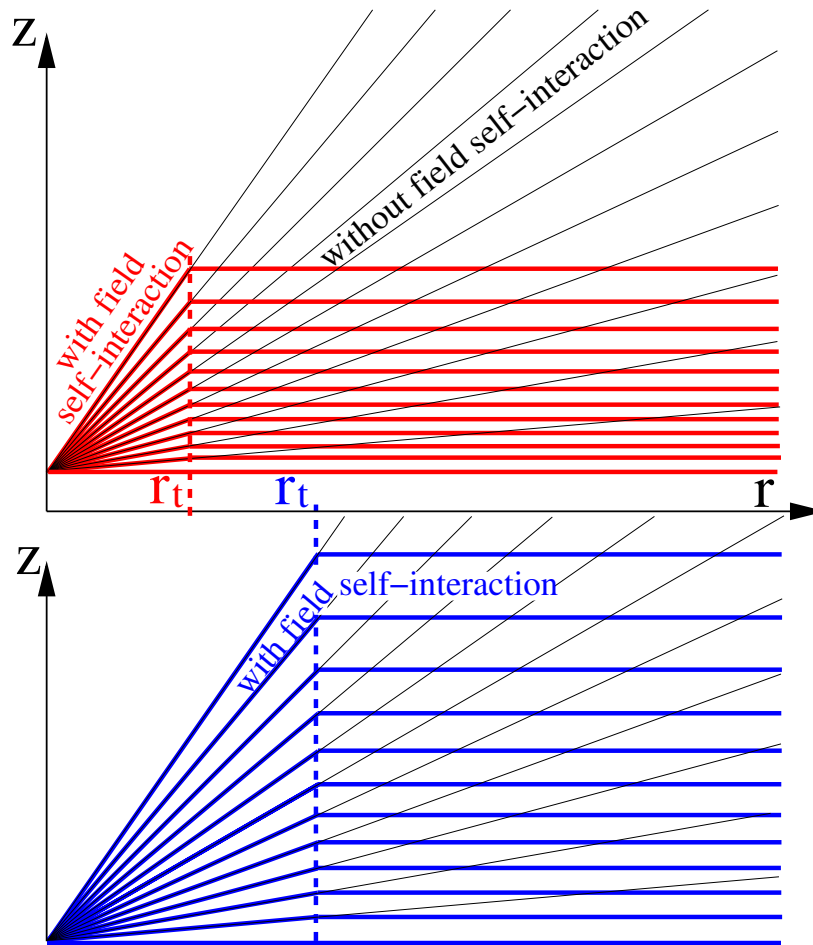


Figure 3. Dependence of G' on the transition scale r_t . Field lines emerge radially for a source (here, for clarity, only those emerging from the galaxy center are shown). A coupling constant, here G' , determines the density of the field lines emerging from the source (or, in this sketch, the number of field lines represented). Since the field possesses energy-momentum, it interacts gravitationally with itself and with masses. Field self-interactions and interactions of the field with the massive disk in the $z = 0$ plane bend the field lines. At smaller r where the field lines are still radially distributed, the force behaves as $1/r^2$ (3D regime). At larger r where they are parallel to each others in a given vertical plane, but are still radially distributed in the disk plane—because of the cylindrical symmetry of the disk—the force behaves as $1/r$ (2D regime). For simplicity, the transition distance between the two regimes is shown here to be infinitely short. For a small r_t (top panel), the field lines at large r are denser. For a larger r_t (bottom panel), the field lines are sparser. Their density is approximately proportional to r_t . Since a force coupling constant reflects the overall density of its field lines (i.e. ignoring the r -dependence) the coupling in the 2D case approximately obeys $G' = G/r_t$ assumed in this article.

dynamically, which may be larger than h_z . Even for an infinitely thin disk ($h_z = 0$), it takes a length r_t for the initially radially distributed field lines to bend into parallel field lines. The mass and its distribution thus determine r_t : the larger the mass and the more concentrated the density, the smaller r_t . The dynamical emergence of r_t in a massive infinitely thin disk is analogous to the emergence of the confinement scale of QCD, or to the energy difference arising between the ground state and first excited levels in atoms or more complex materials in atomic or solid state physics, *viz* computing r_t is a spectral gap problem. The gap problem is notoriously difficult (Carlson et al. 2006) and without known analytical solution. Therefore, even for infinitely thin disks, r_t —or equivalently G' —is non-universal and cannot presently be analytically calculated from first principles. It can be obtained from numerical calculations such as those in Refs. Deur (2009, 2017), or assessed phenomenologically as done in this article.

REFERENCES

Caon, N., Capaccioli, M., & D'Onofrio, M. 1993, MNRAS, 265, 1013, doi: [10.1093/mnras/265.4.1013](https://doi.org/10.1093/mnras/265.4.1013)

Carlson, J., Jaffe, A., & Wiles, A. 2006, The Millennium Prize Problems (American Mathematical Society)

- Clowe, D., Bradač, M., Gonzalez, A. H., et al. 2006, *The Astrophysical Journal*, 648, L109–L113, doi: [10.1086/508162](https://doi.org/10.1086/508162)
- Deur, A. 2009, *Physics Letters B*, 676, 21, doi: [10.1016/j.physletb.2009.04.060](https://doi.org/10.1016/j.physletb.2009.04.060)
- . 2014, *Monthly Notices of the Royal Astronomical Society*, 438, 1535, doi: [10.1093/mnras/stt2293](https://doi.org/10.1093/mnras/stt2293)
- . 2017, *Eur. Phys. J. C*, 77, 412, doi: [10.1140/epjc/s10052-017-4971-x](https://doi.org/10.1140/epjc/s10052-017-4971-x)
- . 2019, *European Physics Journal C*, in press, doi: [10.1140/epjc/s10052-019-7393-0](https://doi.org/10.1140/epjc/s10052-019-7393-0)
- Deur, A., Brodsky, S. J., & de Teramond, G. F. 2016, *Prog. Part. Nucl. Phys.*, 90, 1, doi: [10.1016/j.pnpnp.2016.04.003](https://doi.org/10.1016/j.pnpnp.2016.04.003)
- Einstein, A., Infeld, L., & Hoffmann, B. 1938, *Annals of Mathematics*, 39, 65. <http://www.jstor.org/stable/1968714>
- Graham, A. W., & Worley, C. C. 2008, *MNRAS*, 388, 1708, doi: [10.1111/j.1365-2966.2008.13506.x](https://doi.org/10.1111/j.1365-2966.2008.13506.x)
- Khosroshahi, H. G., Wadadekar, Y., & Kembhavi, A. 2000, *The Astrophysical Journal*, 533, 162, doi: [10.1086/308654](https://doi.org/10.1086/308654)
- Ludlow, A. D., Benítez-Llambay, A., Schaller, M., et al. 2017, *Phys. Rev. Lett.*, 118, 161103, doi: [10.1103/PhysRevLett.118.161103](https://doi.org/10.1103/PhysRevLett.118.161103)
- McGaugh, S. S., Lelli, F., & Schombert, J. M. 2016, *Phys. Rev. Lett.*, 117, 201101, doi: [10.1103/PhysRevLett.117.201101](https://doi.org/10.1103/PhysRevLett.117.201101)
- Méndez-Abreu, J., Aguerri, J. A. L., Corsini, E. M., & Simonneau, E. 2008, *A&A*, 487, 555, doi: [10.1051/0004-6361:20078089e](https://doi.org/10.1051/0004-6361:20078089e)
- Salam, A. 1974, in *IC/74/55*. <http://inspirehep.net/record/90219>
- Sérsic, J. L. 1963, *Boletín de la Asociación Argentina de Astronomía La Plata Argentina*, 6, 41
- Sofue, Y. 2015, *Publications of the Astronomical Society of Japan*, 68, doi: [10.1093/pasj/psv103](https://doi.org/10.1093/pasj/psv103)
- Tully, R. B., & Fisher, J. R. 1977, *A&A*, 54, 661
- Zee, A. 2013, *Einstein Gravity in a Nutshell* (Princeton University Press)